International Journal of Pharmaceutics 361 (2008) 131–140

Contents lists available at ScienceDirect

International Journal of Pharmaceutics

journal homepage: www.elsevier.com/locate/ijpharm

Influence of ageing, grinding and preheating on the thermal behaviour of α-lactose monohydrate

S. Garnier[a,1], S. Petit[a,*], F. Mallet[a,2], M.-N. Petit[a], D. Lemarchand[b], S. Coste[a], J. Lefebvre[c], G. Coquerel[a]

[a] Sciences et Méthodes Séparatives (SMS), UPRES EA 3233, IRCOF – Université de Rouen, F-76821 Mont Saint-Aignan Cedex, France
[b] Groupe de Physique des Matériaux, UMR 6634, Université de Rouen, F-76801 Saint Etienne du Rouvray Cedex, France
[c] Laboratoire de Dynamique des Matériaux Moléculaires, UMR 8024 – Université de Lille 1, F-59655 Villeneuve d'Ascq Cedex, France

ARTICLE INFO

Article history:
Received 1 February 2008
Received in revised form 7 May 2008
Accepted 23 May 2008
Available online 29 May 2008

Keywords:
Dehydration mechanism
Physical pretreatment
Solid–solid transition
Crystal size
α-Lactose monohydrate

ABSTRACT

It is shown that the onset temperature and the magnitude of thermal events observed during DSC analyses of α-lactose monohydrate can be strongly affected by various treatments such as ageing, manual grinding and preheating (cycle of preliminary dehydration and rehydration). In the case of grinding and preheating, the change of dehydration pathways was further investigated by using a suitable combination of characterization techniques, including X-ray powder diffraction (XRPD) performed with a synchrotron source (allowing an accurate Rietveld analysis), scanning electron microscopy (SEM), laser particle size measurements, FTIR spectroscopy and ^{1}H NMR for the determination of β-lactose contents in samples. It appeared that the dehydration mechanism is affected not only by a smaller particle size distribution, but also by residual anisotropic lattice distortions and by the formation of surface defects or high energy surfaces. The fusion–recrystallization process occurring between anhydrous forms of α-lactose at *ca.* 170 °C is not significantly affected by grinding, whereas a preheating treatment induces an unexpected large increase of the enthalpy associated with this transition. Our observations and interpretations confirm the important role of water molecules in the crystal cohesion of the title compound and illustrate the necessity to consider the history of each sample for a satisfactory understanding of the physical properties and the behaviour of this important pharmaceutical excipient.

1. Introduction

The physical characterization of drugs or excipients in the solid state is usually performed by collecting data which constitute the "identity card" of a compound, and is performed by using routine techniques such as X-ray diffraction, DSC and TG, FTIR and Raman spectroscopies, optical and electronic microscopies, etc. (Byrn et al., 1994; Giron, 1995; Brittain, 1999; Vippagunta et al., 2001). This characterization can be completed by supplementary investigations devoted to the stability of the product as a function of its environment, including possible interactions with other components when mixtures or galenic forms are considered (Byrn et al., 1995; Crowley and Martini, 2001). It has also been highlighted in recent research papers and reviews that manufacturing processes such as freeze–drying (Chongprasert et al., 1998), compaction (Fukuoka et al., 1993), grinding (Fukuoka et al., 1995), drying (Hüttenrauch and Keiner, 1979), tabletting (Hüttenrauch, 1983; Shakhtshneider and Boldyrev, 1999), wet granulation, etc. can affect crystal packings and induce physical transformations of solid state samples (Brittain and Fiese, 1999; Morris et al., 2001). Characterization procedures should therefore take into account the preparation route of solid state samples, and investigate the influence of processing on the chemical, physical and thermal stability of samples.

These studies are of particular importance in the case of hydrated or solvated crystalline solids since solvent molecules may contribute significantly to the packing cohesion through intermolecular interactions (Van der Sluis and Kroon, 1989). The dehydration or desolvation mechanisms can range from highly cooperative to destructive–reconstructive (Stephenson et al., 1998; Galwey, 2000), and may depend on experimental conditions (Petit and Coquerel, 1996; Willart et al., 2002). Owing to their struc-

* Corresponding author. Tel.: +33 2 35 52 24 28; fax: +33 2 35 52 29 59.
E-mail address: samuel.petit@univ-rouen.fr (S. Petit).
[1] Present address: Analytical R & D, Novartis Pharma AG, Postfach, CH-4002 Basel, Switzerland.
[2] Present address: GlaxoSmithKline, Gunnels Wood Road, Stevenage, Herts, SG1 2NY, UK.

0378-5173/$ – see front matter © 2008 Elsevier B.V. All rights reserved.
doi:10.1016/j.ijpharm.2008.05.023

tural features (Morris, 1999; Görbitz and Hersleth, 2000), and often in connection with partial or complete desolvations (Stephenson and Diseroad, 2000), solid state properties of hydrates and solvates are therefore more likely to be affected by processes like grinding and drying (Khankari and Grant, 1995; Morris et al., 1998). This statement is nicely illustrated for instance by the case of lactitol hydrates (Yajima et al., 1997; Halttunen et al., 1997).

Among well-known excipients, α-lactose is widely used in the pharmaceutical industry, mainly as a diluent in tablets and capsules (Goodhart, 1994). Either crystalline or amorphous forms of lactose have been extensively studied during the last 35 years, leading sometimes to controversial results or interpretations (Buma, 1978; Kirk et al., 2007). Previous research papers have reported in particular (i) preparation routes, identification and quantification of crystalline/amorphous forms (Buma and Wiegers, 1967; Lim and Nickerson, 1973; Walstra and Jenness, 1984; Angberg, 1995; Figura and Epple, 1995; Fix and Steffens, 2004; Niemelä et al., 2005), (ii) studies on mutarotation in aqueous medium (Walstra and Jenness, 1984) and its influence on nucleation and crystal growth (Dincer et al., 1999; Raghavan et al., 2000, 2001), (iii) structural and morphological investigations (Beevers and Hansen, 1971; Fries et al., 1971; Noordik et al., 1984; Clydesdale et al., 1997; Platteau et al., 2004, 2005; Lefebvre et al., 2005) including the possible influence of structurally related additives (Van Kreveld, 1969; Garnier et al., 2002a), (iv) calorimetric, X-ray diffraction, microscopy and DVS studies on crystallization from amorphous lactose (Berlin et al., 1971; Roos and Karel, 1992; Sebhatu et al., 1994; Darcy and Buckton, 1997; Burnett et al., 2004; Dilworth et al., 2004; Price and Young, 2004; Haque and Roos, 2005), and (v) insights into the dehydration mechanism of α-lactose monohydrate (Figura and Epple, 1995; Garnier et al., 2002b).

The influence on solid state characteristics and thermal behaviour of particle size distribution (Vromans et al., 1985), compressive deformation behaviour (Wong et al., 1991; Busignies et al., 2004), crystallinity (Morita et al., 1984; Di Martino et al., 1993; Bronlund and Paterson, 2004) and physical pretreatments such as grinding, drying and heating (Itoh et al., 1977; Lerk et al., 1984; Irwin and Iqbal, 1991; Otsuka et al., 1991; Longuemard et al., 1998; Willart et al., 2004; Bridson et al., 2007) were also investigated but led in some cases to contradictory conclusions. For instance, several studies (Lerk et al., 1984; Otsuka et al., 1991) have shown that grinding induced both isomerization and 'decrystallization' through mechanical activation (Hüttenrauch et al., 1985) but other authors postulated that changes of DSC curves were only due to a disruption of the water molecule environment within the crystal lattice and/or to the decrease of mean particle size (Irwin and Iqbal, 1991; Longuemard et al., 1998). Crystallinity fluctuations were assumed to be responsible for different physical and thermal properties (Morita et al., 1984; Di Martino et al., 1993), although distinct dehydration behaviours were interpreted by considering only particle size variations, claiming that dehydration is a surface-dependent phenomenon (Vromans et al., 1985). Preheating treatments in organic solvents at the reflux temperature revealed irreversible changes referred to the initial structure (Wong et al., 1991), but the corresponding DSC results were not discussed (Itoh et al., 1977).

In the continuity of our previous work devoted to the dehydration mechanism and to the crystallization of lactose (Garnier et al., 2002b), the present paper reports new insights on the thermal and physical characterization of α-lactose monohydrate (Lα-H_2O) samples as a function of ageing, grinding and preheating (dehydration–rehydration) treatments. A combination of experimental techniques was used in order to elaborate reliable interpretations.

2. Material and methods

2.1. Preparation of samples

Commercial α-lactose monohydrate (Acros, 99.5%) was purified and gently recrystallized according to a procedure described elsewhere (Garnier et al., 2002a,b). After filtration by suction, solid state samples were dried under a ventilated atmosphere at room temperature from 24 h ("freshly recrystallized" samples) to several weeks ("aged" samples). Hereafter, initial Lα-H_2O depicts our starting material, and consists of freshly recrystallized samples dried in room conditions during 3–5 days.

Manual grinding was carried out with a pestle and mortar for increasing periods of time (20 min, 120 min, 300 min). Further grinding was shown to have no influence.

Thermal pretreatments were performed by maintaining non ground Lα-H_2O samples at 130 °C for 3 h in order to produce the dehydrated $L\alpha_H$ form (Garnier et al., 2002a). Complete rehydration occurred at room temperature within three days under atmospheric humidity. Both dehydration and rehydration were monitored by gravimetry.

2.2. Characterization techniques

Routine X-ray powder diffraction (XRPD) patterns were collected on a Siemens D5005 diffractometer (Cu Kα, λ = 1.5418 Å). High-quality XRPD patterns were obtained with a synchrotron source at the ESRF, Grenoble (France) on the BM16 line (Dr. A. Fitch). The selected wavelength was 0.949531 Å, with 5 min exposure. Owing to the quality of these measurements, no background correction was applied.

The synchrotron X-ray patterns ($1.03^\circ < 2\theta < 27.98^\circ$, 2θ step = 0.005°) were analyzed using the Le Bail method (Le Bail et al., 1988) implemented in FULLPROF (Rodriguez-Carvajal, 2001) interfaced by the WinPLOTR graphic software (Roisnel and Rodriguez-Carvajal, 2001), and taking into account the instrumental resolution function. This function was obtained through a Le Bail whole-powder-pattern profile refinement using a powder pattern of a standard compound ($Na_2Ca_3Al_2F_{14}$, NAC) in the angular range 7.0–41.9° (2θ). The Bragg peak profiles (Thompson–Cox–Hastings function; Thompson et al., 1987) were found to be both Gaussian and Lorentzian, and the full width at half-maximum (FWHM) to have an angular dependence given by:

$$H_G = U\tan^2\theta + V\tan\theta + W \quad \text{with} \quad U = 0.00091(5),$$

$$V = -0.00051(2) \quad \text{and} \quad W = 0.000080(1)$$

$$H_L = X\tan\theta + \frac{Y}{\cos\theta} \quad \text{with} \quad X = 0 \quad \text{and} \quad Y = 0.00799(2)$$

In order to determine the microstructural effects generated by grinding and preheating, the peak-shape function, a Thompson–Cox–Hastings profile function was used (Thompson et al., 1987). The best refinement has been obtained by using isotropic size effects and anisotropic strain effects (Stephens, 1999). The number of fitted parameters was 34 (four cell parameters, two asymmetry corrections, one zero-shift, 17 background points (16 for 300 min), nine anisotropic strain parameters and one Lorentzian strain coefficient (for 300 and 0 min) and 1 *Y* parameter (for 300 and 120 min).

DSC experiments were carried out using a Setaram 141 apparatus with a constant 2 K/min heating rate, from 30 °C to 200 °C. Non sealed aluminium crucibles were used in order to allow a free water escape during dehydration. When required, simultaneous TG/DSC measurements were performed in identical conditions, using a Netzsch STA 409 PC apparatus.

Native and ground or preheated samples were observed by SEM using a LEO 1530 apparatus at various magnifications.

Crystal size distribution of solid state samples was evaluated by using a laser particle size analyzer (LS 230, Beckman Coulter). Lα-H_2O samples were dispersed in $CHCl_3$ and each stirred suspension was submitted to measurement during 90–100 s. The presence of very small particles (from 0.04 μm to 1 μm) was estimated using the integrated PIDS module.

FTIR spectroscopy measurements were carried out with a Paragon 500 (Perkin Elmer) apparatus. Samples were conditioned in dry KBr disks and spectra were collected from 400 cm^{-1} to 4000 cm^{-1} with an instrumental resolution of 2 cm^{-1}.

^1H NMR spectra were collected with a Bruker Avance system (300 MHz) in deuteriated DMSO. In this solvent, mutarotation of lactose (α-lactose ↔ β-lactose) occurs very slowly (Dincer et al., 1999), so proportions of the two anomeric forms could be accurately determined by using a procedure described elsewhere (Willart et al., 2004).

3. Results and discussion

3.1. Influence of ageing

The DSC curves in Fig. 1 allow the comparison between the thermal behaviour of freshly recrystallized Lα-H_2O (analyzed less than 24 h after filtration) and that of aged Lα-H_2O (analyzed more than three weeks after filtration). The large endothermic phenomenon at *ca.* 130 °C (onset temperature) corresponds to the dehydration of Lα-H_2O towards the hygroscopic anhydrous phase ($L\alpha_H$), and presents similar shapes and enthalpies in the two curves. Between 160 °C and 180 °C, a double endothermic–exothermic phenomenon can be observed, but its magnitude decreases continuously with ageing (for the endothermic part, *ca.* 14 J/g after 24 h, 8 J/g after 7 days, 2 J/g after 3 weeks, 1.5 J/g after 4 weeks or more). These weak thermal events were previously interpreted as a polymorphic transformation between hygroscopic ($L\alpha_H$) and stable ($L\alpha_S$) anhydrous forms of α-lactose (Garnier et al., 2002b). However, this double phenomenon has not been observed in numerous previous studies (Vromans et al., 1985; Otsuka et al., 1991), or has been detected only when using form $L\alpha_H$ as starting material (Figura and Epple, 1995).

This first result shows to which extent the thermal behaviour of Lα-H_2O can be sensitive to the preparation of the sample and to operating conditions. It can be assumed that the reason why the $L\alpha_H \rightarrow L\alpha_S$ transformation was not or only partially detected in previous studies is due not only to the weakness of the heat flows,

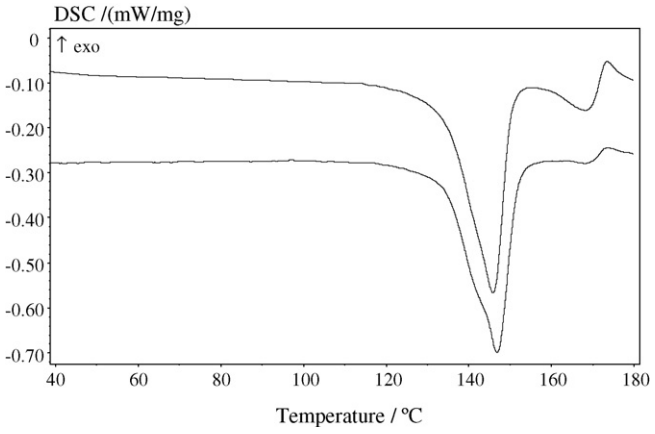

Fig. 1. DSC curves of freshly recrystallized Lα-H_2O, dried under ventilated atmosphere for less than 24 h (upper) and aged more than three weeks (lower).

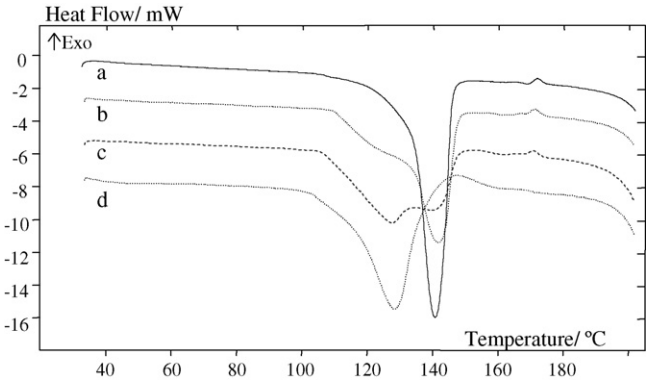

Fig. 2. DSC curves of initial and ground samples of Lα-H_2O ((a) initial; (b) 20 min; (c) 120 min; (d) 300 min).

but also to the delay between the preparation of the samples and their analysis.

The decrease upon ageing of the heat exchange associated with this transformation probably results from the existence of two opposite (endo- and exothermic) contributions, probably corresponding to a fusion and recrystallization process. The apparent decrease of the associated enthalpy may actually be the consequence of an increasing overlap of the two thermal events, caused by a progressive decrease of the onset temperature for the exothermic phenomenon (recrystallization). Factors that may explain this decrease are the progressive release of residual water upon ageing and the slow relaxation of Lα-H_2O crystals. For instance, the completeness of the drying process in a ventilated atmosphere could affect the dehydration process itself, leading to $L\alpha_H$ crystals with different particle size distributions and/or crystallinities (Petit and Coquerel, 1996). The change in proportion and location of crystal defects in $L\alpha_H$ may also have an impact on the subsequent transformation (Mnyukh, 1979).

3.2. Influence of grinding

It can be seen from Fig. 2 that the thermal behaviour of Lα-H_2O is deeply affected by grinding. The narrow DSC peak associated with dehydration of the initial sample (onset *ca.* 132 °C) is progressively replaced by a distinct thermal event starting at about 105 °C. The curve obtained after 120 min of grinding clearly demonstrates the existence of two distinct dehydration peaks. Furthermore, the continuous decrease in magnitude of the initial dehydration peak with the increase of the new peak at lower temperature indicates a change of the dehydration mechanism of ground Lα-H_2O but does not lead to a different crystalline variety since the resulting phase is still $L\alpha_H$ solely (checked by conventional XRPD).

From a previous analysis of Lα-H_2O crystal structure, we had postulated that the departure of water molecules from the 3D packing should occur along independent structural channels parallel to the crystallographic *c*-axis (Garnier et al., 2002b). The sudden decrease by about 30 °C of the dehydration temperature reveals that manual grinding may generate new pathways for the evacuation of water molecules. It could be envisaged, for instance, that channels are not anymore independent in ground material, inducing that water molecules have more degrees of freedom during their evacuation and become less sensitive to defects that could block the channels.

The appearance of new dehydration pathways is therefore due to the structural and macrocrystalline consequences of manual grinding. Various physical factors may be involved since grinding could simultaneously induce:

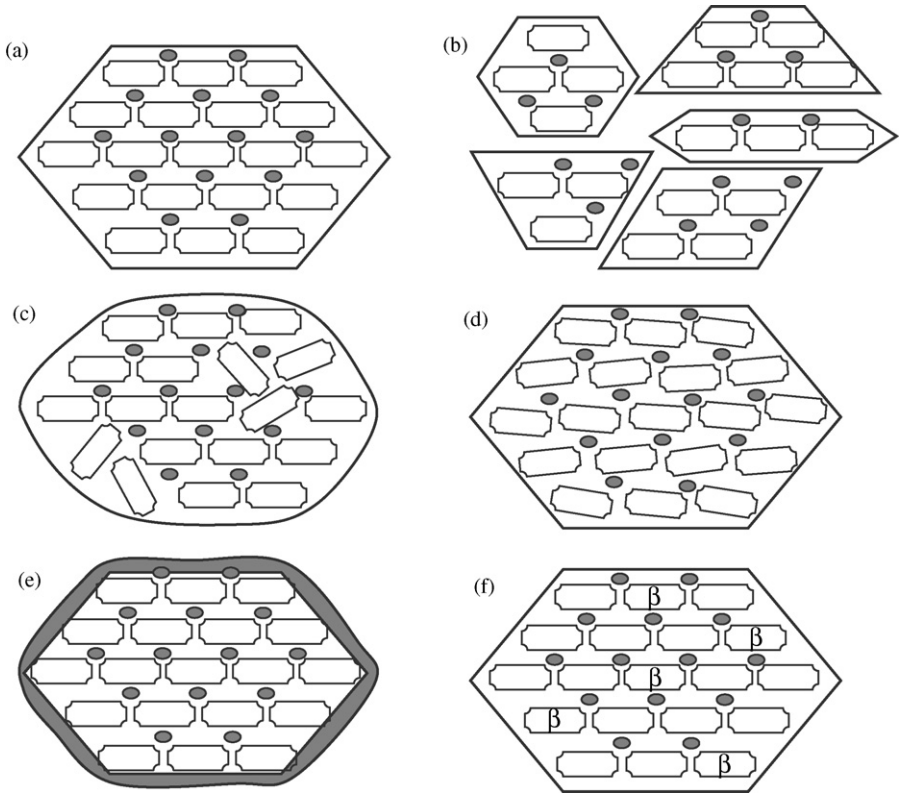

Fig. 3. Simplified representation of hypothetical structural and macrocrystalline consequences of manual grinding of Lα-H_2O ((a) idealized initial packing; (b) decrease of particle size; (c) sharp increase in the number of crystal defects; (d) anisotropic lattice distortions; (e) amorphous layer at surfaces; (f): mutarotation in the solid state).

- a decrease of the mean particle size (probably with anisotropic cleavage directions),
- the formation of crystal defects in the crystal lattice (0D or 1D) and the disruption of intermolecular hydrogen bonds,
- some anisotropic distortions of the 3D lattice,
- the formation of an amorphous (or ill-crystallized) layer mainly at the surface of particles (Chikhalia et al., 2006),
- an increase of the proportion of β-lactose molecules.

Considering as a reference an ideal crystal packing without any defect, a schematic representation of each of these parameters is shown in Fig. 3, and it should be kept in mind that their simultaneous occurrence may result in synergetic effects that could make them difficult to characterize individually.

Changes in crystal size distribution, putative partial amorphization and anisotropic lattice distortions were investigated from high-quality XRPD patterns collected with a synchrotron source (Fig. 4). The absence of new diffraction peaks and the background profile indicate that no solid–solid transformation occurs upon grinding, and confirms that the Lα-H_2O phase remains highly crystalline.

The progressive decrease of peak intensities and their simultaneous broadening was assumed to be due to the decrease of the mean particle size, which was confirmed by simulations of XRPD patterns at different crystal size, through a Scherrer's fit (Azároff and Buerger, 1958). Despite the assumption, in this first approach, of an isotropic decrease of particle size, a satisfactory agreement

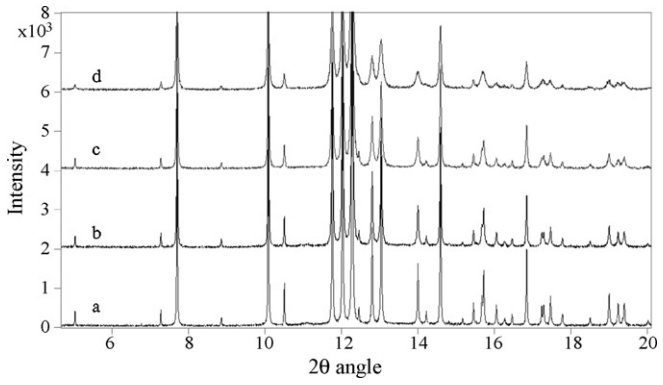

Fig. 4. XRPD patterns (synchrotron source, λ = 0.949531 Å) of initial and ground samples of Lα-H_2O ((a) initial; (b) 20 min; (c) 120 min; (d) 300 min).

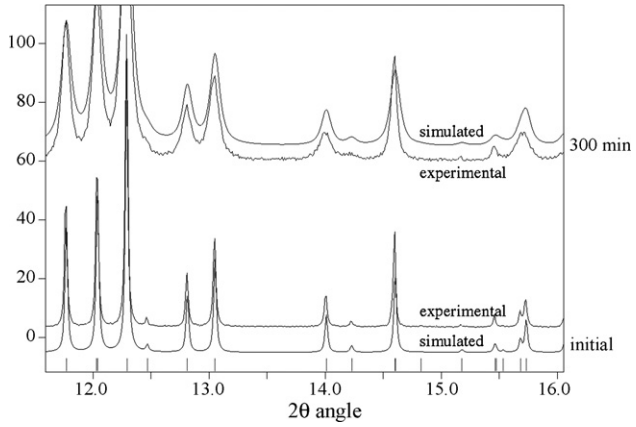

Fig. 5. Superimposition of experimental XRPD patterns with that simulated with different values of particle size μ (lower: initial sample, μ = 2000 Å; upper: ground for 300 min, μ = 550 Å).

Table 1
Main results of the Rietveld refinements of synchrotron XRPD patterns achieved with the FULLPROF software

Grinding time (min)	0	20	120	300	Dehydrated– rehydrated
Lorentzian strain coefficient	0.74(2)	0.75	0.82	0.68(2)	0.259(11)
Anisotropy strain $\times 10^{-4}$	9.1968 (1.6518)	14.7704 (3.0355)	23.1609 (7.1417)	36.0632 (14.9247)	44.6801 (15.8406)
a (Å)	7.93933(5)	7.93886(7)	7.9390(1)	7.9391(1)	7.9399(2)
b (Å)	21.5780(1)	21.5770(1)	21.5785(2)	21.5851(4)	21.5994(4)
c (Å)	4.81594(3)	4.81575(4)	4.81602(5)	4.81691(9)	4.8116(2)
β (°)	109.7671(4)	109.7653(5)	109.7605(8)	109.758(1)	109.694(2)
R_p	12.3	11.8	11.7	10.7	13.5
R_{wp}	15.7	15.0	14.8	14.7	15.2
R_{exp}	8.23	8.50	8.48	8.33	11.1
χ^2	3.66	3.13	3.03	3.10	1.87
R_B	0.5×10^{-4}	0.0028	0.029	0.0056	0.017
R_F	0.97×10^{-4}	0.0041	0.036	0.0074	0.02

was obtained from these simulations (Fig. 5), and it could be estimated that the mean crystal size is decreased approximately by a factor 4 by considering the two extreme situations (initial Lα-H_2O sample and Lα-H_2O ground for 300 min).

A more detailed analysis of XRPD patterns was performed through Rietveld refinements, using FULLPROF (Table 1). This analysis could not confirm the estimated ratio of decrease of apparent particle size, due to missing values for initial Lα-H_2O and for the sample ground for 20 min However, beside the evolution of CSD, Table 1 reveals a continuous increase of the anisotropy strains from *ca.* 0.09% to 0.36% upon grinding. The directions of this limited but progressive lattice distortion can be visualized in Fig. 6, indicating that the main residual deformations are running along bisectors of (*a*, *c*) and (*b*, *c*) axes, whereas the weakest remaining strains are observed along the three crystallographic axes.

These data can be discussed in view of the H-bonding network existing in the crystal structure of Lα-H_2O, since previous structural descriptions (Fries et al., 1971; Noordik et al., 1984; Clydesdale et al., 1997; Garnier et al., 2002a; Platteau et al., 2004) have shown that the strongest periodic bond chains (PBCs) are running along the three main crystallographic directions. As a consequence, the crystal packing may exhibit a weaker elastic character (and probably a brittle character) along these axes, whereas bisectors are more likely to undergo lattice distortions, associated with the appearance, at a lower energetic cost, of crystal defects.

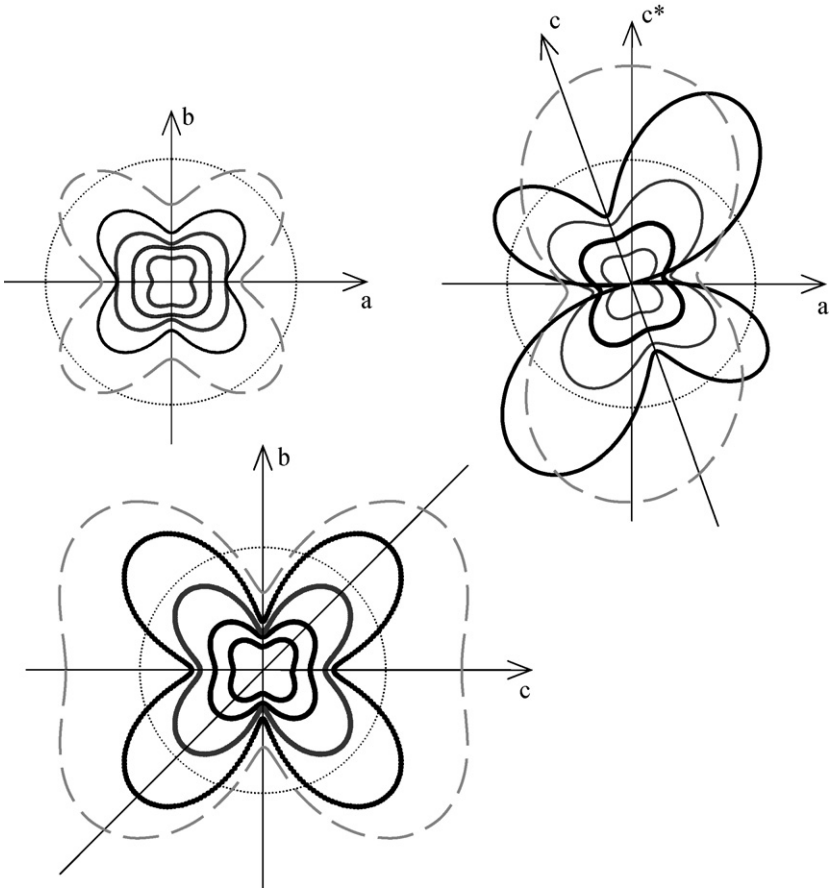

Fig. 6. Anisotropic distortion profiles of the crystal lattice as deduced from the analysis of powder patterns obtained from Le Bail refinements (by increasing size: initial Lα-H_2O; ground 20 min; 120 min; 300 min). The dashed curves correspond to the dehydrated–rehydrated sample. The circle depicts a distortion of 0.36%.

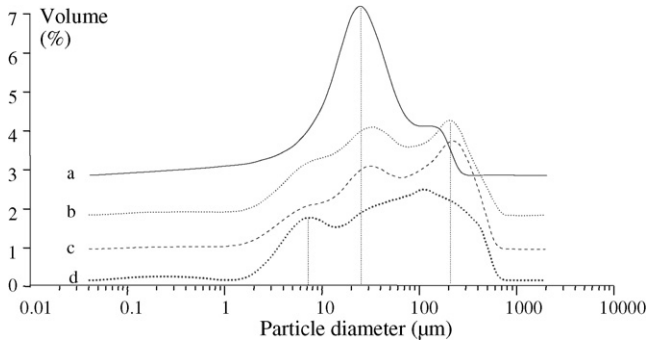

Fig. 7. Crystal size distribution of initial and ground Lα-H_2O ((a) initial; (b) 20 min; (c) 120 min; (d) 300 min).

Hence, the analysis of residual lattice distortions from high-quality XRPD patterns indicates that manual grinding produces a highly anisotropic deformation of the crystal packing affecting predominantly directions of weakest cohesion energy. Since strain effects are known to be caused by crystal defects (Platteau et al., 2004), it can be expected that grinding actually induces the breaking of H-bonds (lactose–lactose or lactose–water bonds), and this partial disruption of the H-bonding network may contribute to explain the easier departure of water molecules and the lower dehydration activation energy, as revealed by DSC analyses. Moreover, it can be postulated that H-bond disruptions may affect a larger proportion of lactose–water bonds, referred to lactose–lactose contacts, since it was shown previously, using molecular modeling tools that direct lactose–lactose H-bonds contribute more strongly to the energetic cohesion in the packing of Lα-H_2O than lactose–water interactions (Clydesdale et al., 1997).

The physical characterization of initial and ground Lα-H_2O samples was completed by CSD measurements with a laser granulometer and by SEM observations. The CSD curves shown in Fig. 7 indicate that the homogeneous distribution (mean diameter 20–30 μm) of the initial sample is transformed upon grinding into a more complex distribution, with a bi-modal population of particles in the ranges 5–9 μm and 150–300 μm. It is noteworthy that an analogy can be highlighted between the DSC curves and the evolution of the mean particle size from *ca.* 25 μm to *ca.* 7 μm. In both cases, one can indeed contemplate a jump from the starting situation to the final state, instead of a continuous shift of DSC peaks or crystal size of the smallest particles. This statement confirms the predominant roles of defects and crystal size distribution in the dehydration mechanism, probably related to the necessary diffusion of water molecules along suitable pathways. In the present case, it is likely that a 'low energy' grinding allows the formation of defective particles of homogeneous size, from which water molecules can be evacuated more easily through anisotropic pathways. The relevance of a size effect is confirmed by the ratio of particle size decrease (*ca.* a factor four from 25 μm to 7 μm) since this ratio is close to that deduced from the Scherrer analysis of XRPD patterns. The appearance of a population of larger CSD (150–300 μm) during manual grinding may be due to an agglomeration effect of ground particles caused by friction forces, welding or electrostatic effects that probably increase the surface energy of powder particles (Kumon et al., 2006).

The formation of very small particles with a rounded shape was confirmed by SEM observations (Fig. 8), and is consistent with the appearance of an ill-crystallized superficial layer on Lα-H_2O particles. The analysis of initial and ground samples by FTIR spectroscopy led to very similar spectra (data not shown). The only detectable evolution induced by grinding is the presence of large amounts of adsorbed water at the surface of particles (in the region 3700–3900 cm^{-1}), probably in connection with the existence of ill-defined surfaces for ground samples.

Since previous studies have shown that intensive grinding of Lα-H_2O induces an isomerization in the solid state (Lerk et al., 1984; Otsuka et al., 1991), proportions of β-lactose molecules in initial and ground samples were determined by ^1H NMR at room temperature and after heating up to 180 °C at the 2 °C/min heating rate. It should be noticed that the presence of β-lactose molecules is not associated with the formation of Lβ or Lα/β crystals (checked by XRPD) but corresponds to a solid solution in Lα phases (Raghavan et al., 2000).

It can be seen from Table 2 that manual grinding is responsible for a significant increase of the proportion of β-lactose molecules in the crystal lattice of Lα-H_2O at room temperature, and this could be an additional reason for the formation of crystal defects and lattice distortions depicted above.

Upon heating from room temperature up to 180 °C, the proportion of β-lactose is higher for native material than for ground samples, which can be explained by the decrease of the dehydration temperature caused by grinding since this decrease induces a shorter residence time of H_2O molecules in the crystal lattice upon heating. Previous studies have shown that mutarotation produced by ball milling is much weaker than that induced by thermal treatments (Willart et al., 2004), and the amount of β-lactose obtained upon heating is probably sensitive to the presence of residual water. We have shown in a previous study that water released by dehydration of large crystals (*ca.* 500 μm) in stagnant methanolic conditions was able to induce the mutarotation and leads to the formation of macroscopic crystals of anhydrous β-lactose (Garnier et al., 2002b). In the present case, the lower proportion of β-lactose molecules formed during dehydration of ground samples is likely to be due to the combined effect of smaller particles (and therefore lower amounts of released water per particle) undergoing an easier dehydration at lower temperature. Therefore, the more rapid release of water from ground Lα-H_2O, the weaker the catalytic effect of dehydration on the mutarotation equilibrium.

Hence, the decrease by about 30 °C of the dehydration temperature caused by manual grinding results from the formation of a new population of particles with a smaller mean size associated to the appearance of new pathways, allowing an easier diffusion of water molecules upon heating. This jump towards different dehydration pathways is the consequence of several changes of physical parameters affecting the structural and macrocrystalline cohesion of Lα-H_2O. In particular, the discontinuous reduction of the mean particle size, the anisotropic distortion of the crystal lattice, the formation of crystal defects or lattice disruptions and the formation of ill-crystallized layers at the surface of particles may account for the considerable change of Lα-H_2O dehydration mechanism. In contrast with 'hard' milling conditions that are known to induce large amorphous contents (Otsuka et al., 1991; Willart et al., 2004), the 'soft' manual grinding applied in the present study does not lead to significant proportions of amorphous lactose but, owing to the effects depicted above, seems to constitute an intermediate step of the 'decrystallization' process that may progressively generate an amorphous solid.

3.3. Influence of preheating (dehydration–rehydration)

Under suitable conditions, the dehydration of Lα-H_2O can reversibly lead to the hygroscopic $L\alpha_H$ phase (Figura and Epple, 1995). Nevertheless, the thermodynamic reversibility is not necessarily associated with reversibility in terms of dehydration mechanism or molecular process. In order to study the influence of a preliminary cycle of dehydration/rehydration on the thermal behaviour of Lα-H_2O, a sample

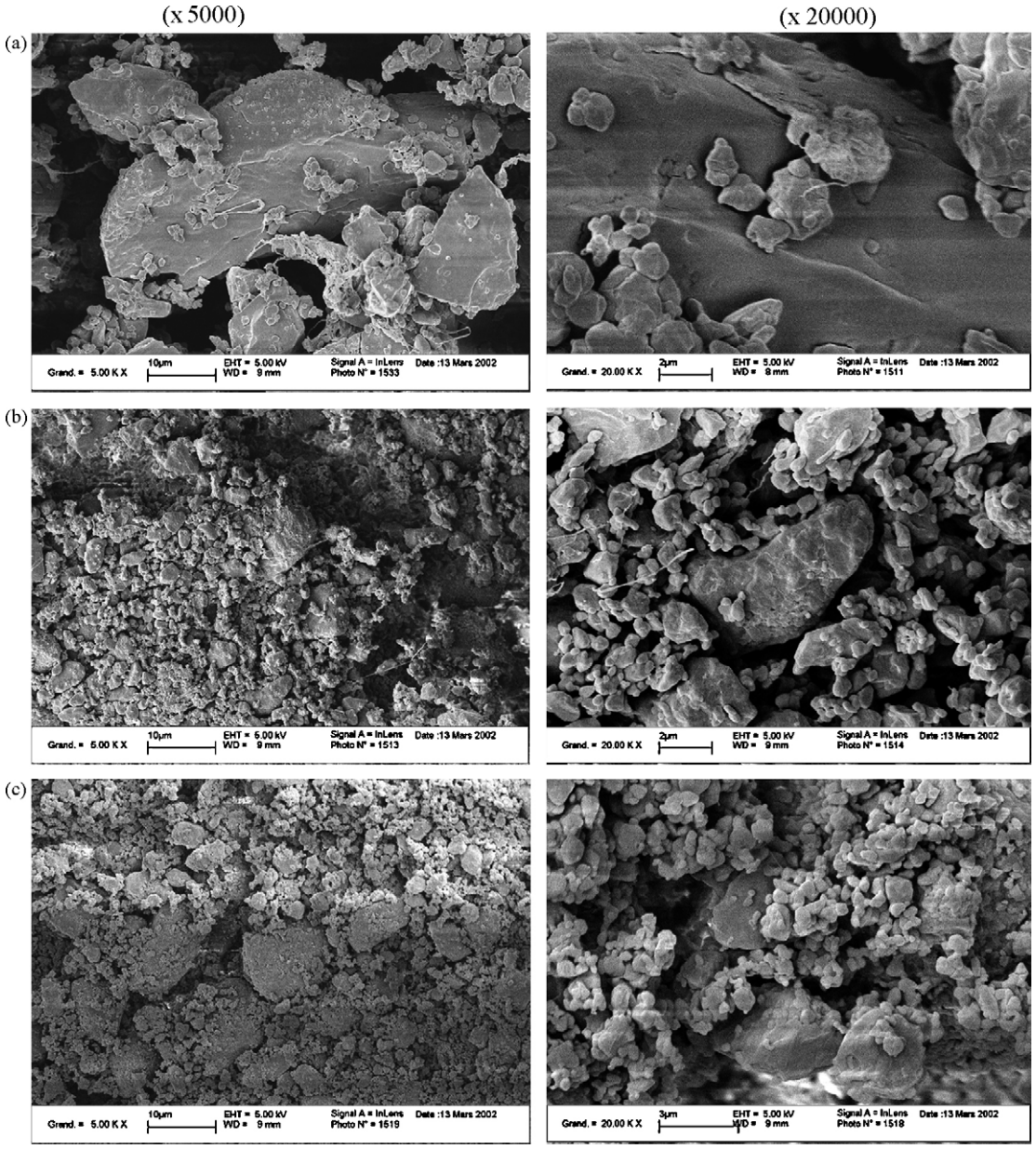

Fig. 8. SEM photographs of initial and ground Lα-H_2O ((a) initial; (b) 20 min; (c) 300 min). Magnification is ×5000 (left) and ×20,000 (right).

was maintained at 130 °C during 3 h and was allowed to rehydrate at room temperature under ambient humidity for at least three days. These two processes (dehydration and rehydration) were monitored by means of gravimetric measurements (5.0 ± 0.2% of weight change) and conventional XRPD identification (Buma and Wiegers, 1967). Initial and preheated samples were then characterized using a combination of relevant techniques.

Fig. 9 presents the superimposition of DSC curves obtained for initial Lα-H_2O, rehydrated Lα-H_2O and $L\alpha_H$. For the 'dehydrated' phase $L\alpha_H$, a small endothermic phenomenon is observed at *ca.* 100 °C, revealing that rehydration has already partially occurred. More surprisingly, the endo/exothermic phenomenon corresponding to the $L\alpha_H \rightarrow L\alpha_S$ transformation starts at lower temperature than for the initial material (onset at *ca.* 160 °C), with a greater magnitude. Since the temperature of the exothermic part does not seem to be affected by preheating, it is likely that, as in the case of ageing (see Section 3.1), the larger apparent enthalpy results from the decrease in temperature of the endothermic contribution, inducing a better resolution of the two thermal effects.

Compared to the initial Lα-H_2O sample, the DSC curve of rehydrated Lα-H_2O exhibits unexpected changes.

Table 2
Proportions of β-lactose molecules in Lα-H_2O samples at 20 °C and after heating up to 180 °C at 2 °C/min

Temperature (°C)	Native Lα-H_2O (%)	Ground Lα-H_2O (300 min) (%)	Preheated Lα-H_2O (dehydrated–rehydrated) (%)
20	2.5	4.0	6.5
180	23.6	13.1	24.9

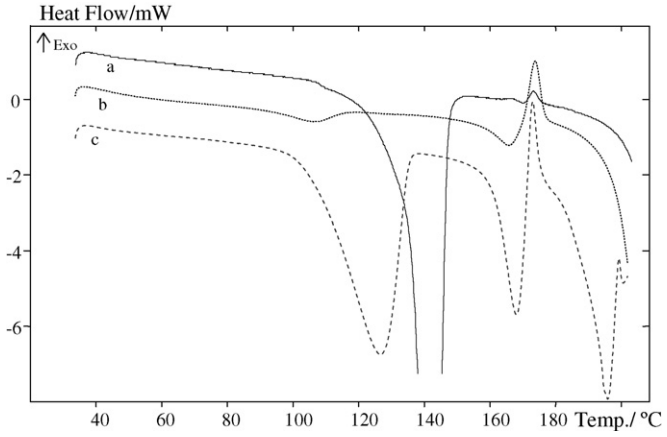

Fig. 9. DSC curves of initial and preheated Lα-H_2O ((a) initial; (b) dehydrated-$L\alpha_H$; (c) dehydrated/rehydrated).

- First, the dehydration peak becomes broader, and the onset temperature is lowered to *ca.* 105 °C. Nevertheless, the shape of this phenomenon clearly differs from that obtained for ground Lα-H_2O (Fig. 2), and the associated enthalpy decreases by about 10%.
- The second unexpected difference concerns the $L\alpha_H \rightarrow L\alpha_S$ pathway at 160 °C. For native Lα-H_2O, the two events are difficult to distinguish due to extensive overlapping. For rehydrated Lα-H_2O the two thermal events are now clearly decoupled. The first thermal event is associated with a large heat exchange, corresponding approximately to one third of the dehydration enthalpy. It is interpreted as the (endothermic) metastable fusion of $L\alpha_H$ rapidly followed by the (exothermic) recrystallization of $L\alpha_S$.

After the double phenomenon, fusion/decomposition of $L\alpha_S$ can be observed from *ca.* 180 °C upwards, starting therefore about 20 °C before that of initial Lα-H_2O. As for ground Lα-H_2O, DSC analysis indicates that a thermal pretreatment generates new pathways for the dehydration process, inducing here that the physical properties of the dehydrated material ($L\alpha_H$) impact the subsequent $L\alpha_H \rightarrow L\alpha_S$ pathway.

High-quality XRPD patterns of initial and preheated Lα-H_2O are shown in Fig. 10, revealing an important decrease of peak intensities with a very limited amount of amorphous material, if any, and no other crystallized phase. Nevertheless, the computation, using the modelling software Cerius[2], of XRPD patterns simulating the influence of an isotropic decrease of mean particle size leads to significant discrepancies between measured and calculated peak intensities (data not shown). This indicates that the dehydration/rehydration process occurs in a highly anisotropic way, as anticipated earlier (Garnier et al., 2002b).

The comparative analysis of XRPD patterns by Rietveld refinements with FULLPROF (Table 1) shows that the mean anisotropic lattice distortions produced by preheating are more pronounced (0.44%) than that resulting from grinding (0.36%), despite a larger apparent crystal size (4690(4) Å for preheated Lα-H_2O *vs.* 1860(2) Å for Lα-H_2O ground during 300 min). Interestingly, the distortion profiles (Fig. 6) indicate that large residual distortions are observed along the c^*-direction, *i.e.* running parallel to structural channels along which water molecules are assumed to be preferentially evacuated during a cooperative dehydration. Therefore, data presented here are consistent with our previous interpretation of the dehydration process at a molecular scale (Garnier et al., 2002b), and the anisotropic character of a preliminary dehydration–rehydration

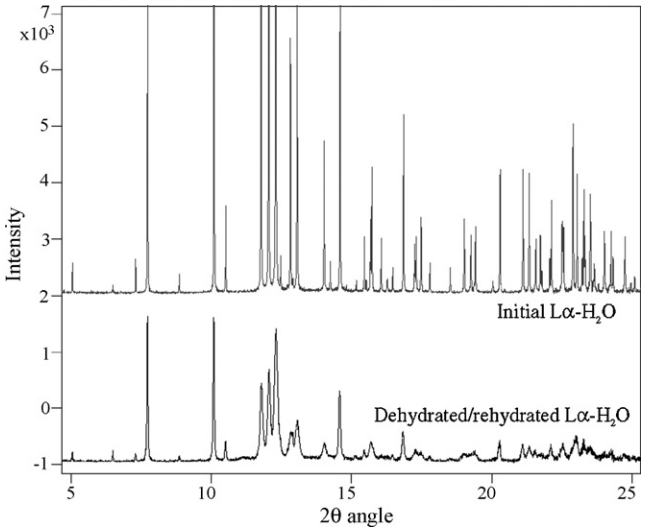

Fig. 10. XRPD patterns (synchrotron source, λ = 0.949531 Å) of initial (upper) and dehydrated/rehydrated (lower) samples of Lα-H_2O.

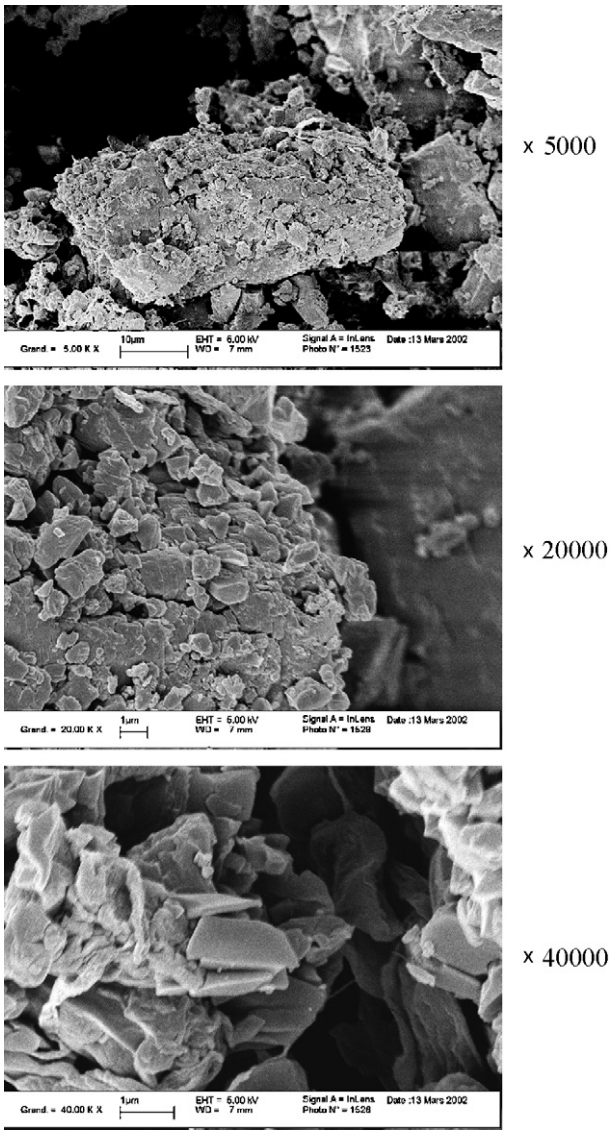

Fig. 11. SEM photographs of dehydrated/rehydrated Lα-H_2O samples with increasing magnification.

differs to a certain extent from the consequences of a mechanical pretreatment.

Further characterization of preheated Lα-H_2O samples by scanning electron microscopy (Fig. 11) indicate that a large number of small particles (1 μm to 10 μm) are produced by the preliminary dehydration–rehydration, in agreement with data obtained from laser particle size measurements (data not shown). At high magnification (×40,000), SEM examination of a preheated Lα-H_2O sample revealed the existence of flat and well-defined morphologies that clearly differ from ill-defined round shapes generated by grinding (Fig. 8). FTIR spectroscopy did not allow the detection of differences between initial and preheated Lα-H_2O (data not shown), but determinations of β-lactose contents at room temperature and at 180 °C (Table 2) indicated that preheating leads to a significant mutarotation ratio, inducing that the proportion of β-lactose molecules at 180 °C is slightly superior to that obtained for native samples, despite a lower dehydration temperature. The formation of domains made of a stoichiometric α:β = 1:1 molecular compound could be envisaged, but is not expected in the present case since this compound could only be crystallized by heating amorphous lactose (Lefebvre et al., 2005; Lefort et al., 2006).

Hence, the preheating treatment appears to have structural and physical consequences differing from that produced by manual grinding, and these distinct dehydration pathways may in turn be responsible for the decrease of the onset temperature for the irreversible evolution $L\alpha_H \rightarrow L\alpha_S$.

4. Conclusion

Mechanical (manual grinding) or thermal (dehydration–rehydration) pretreatments can deeply affect the thermal behaviour of crystalline Lα-H_2O. In particular, the decrease by about 30 °C of the dehydration temperature appears to be associated with a profound change in dehydration pathways. Both treatments induce an important (and discontinuous) decrease of the mean particle size, as well as significant residual anisotropic lattice distortions that constitute an intermediate step of an amorphization process. These physical changes account for the direct jump from an initial material to a new population exhibiting a lower dehydration temperature. Manual grinding also produces particles with a rounded shape and irregular surfaces inducing that friction or electrostatic forces may be involved in the change of dehydration mechanism. For ground samples, the limited mutarotation ratio can be understood in terms of lower residence time of water molecules within lactose particles upon heating. In the case of a preliminary dehydration–rehydration cycle, surfaces are less affected but the large lattice distortions in the direction of channels along which water molecules are evacuated lead to a lower onset temperature and to a decoupling of the fusion ($L\alpha_H$)–recrystallisation ($L\alpha_S$) processes.

These interpretations are consistent with the large contribution of water molecules to the structural cohesion of Lα-H_2O, and highlight that, for hydrates and solvates, the history of a given sample should be taken into account in order to elucidate their behaviour and to rationalize the data collected during their solid state characterization.

Acknowledgements

Thanks are due to: (i) Dr. Valérie DUPRAY (University of Rouen, site of Evreux) for particle size measurements, (ii) European Synchrotron Radiation Facilities (ESRF, Grenoble, France) for access to BM16 (Dr. Andy FITCH) and (iii) CRIHAN (Centre de Ressources Informatiques de Haute-Normandie, Rouen) for providing access to the Cerius^2 molecular modeling software (Accelrys Inc.).

Interreg IIIA network (EU fundings) is acknowledged for its support to this study.

References

Angberg, M., 1995. Lactose and thermal analysis with special emphasis on microcalorimetry. Thermochim. Acta 248, 161–176.
Azároff, L.V., Buerger, M.J., 1958. The Powder Method in X-ray Crystallography. McGraw-Hill, New York, pp. 254–266.
Beevers, C.A., Hansen, H.N., 1971. The structure of α-lactose monohydrate. Acta Crystallogr. B27, 1323–1325.
Berlin, E., Kliman, P.G., Anderson, B.A., Pallansch, M.J., 1971. Calorimetric measurements of the heat of desorption of water vapor from amorphous and crystalline lactose. Thermochim. Acta 2, 143–152.
Bridson, R.H., Robbins, P.T., Chen, Y., Westerman, D., Gillham, C.R., Roche, T.C., Seville, J.P.K., 2007. The effects of high shear blending on α-lactose monohydrate. Int. J. Pharm. 339, 84–90.
Brittain, H.G., 1999. Methods for the characterization of polymorphs and solvates. In: Brittain, H.G. (Ed.), Polymorphism in Pharmaceutical Solids, 95. Marcel Dekker, New York, pp. 227–278.
Brittain, H.G., Fiese, E.F., 1999. Effects of pharmaceutical processing on drug polymorphs and solvates. In: Brittain, H.G. (Ed.), Polymorphism in Pharmaceutical Solids, vol. 95. Marcel Dekker, New York, pp. 331–361.
Bronlund, J., Paterson, T., 2004. Moisture sorption isotherms for crystalline, amorphous and predominantly crystalline lactose powders. Int. Dairy J. 14, 247–254.
Buma, T.J., 1978. Lactose obtained by crystallization from methanol. Neth. Milk Dairy J. 32, 258–261.
Buma, T.J., Wiegers, G.A., 1967. X-ray powder patterns of lactose and unit cell dimensions of β-lactose. Neth. Milk Dairy J. 21, 208–213.
Burnett, D.J., Thielmann, F., Booth, J., 2004. Determining the critical relative humidity for moisture-induced phase transitions. Int. J. Pharm. 287, 123–133.
Busignies, V., Tchoreloff, P., Leclerc, B., Besnard, M., Couarraze, G., 2004. Compaction of crystallographic forms of pharmaceutical granular lactoses. Eur. J. Pharm. Biopharm. 58, 569–576.
Byrn, S.R., Pfeiffer, R.R., Stephenson, G., Grant, D.J.W., Gleason, W.B., 1994. Solid-state pharmaceutical chemistry. Chem. Mater. 6, 1148–1158.
Byrn, S.R., Pfeiffer, R.R., Ganey, M., Hoiberg, C., Poochikian, G., 1995. Pharmaceutical solids: a strategic approach to regulatory considerations. Pharm. Res. 12, 945–954.
Chikhalia, V., Forbes, R.T., Storey, R.A., Ticehurst, M., 2006. The effect of crystal morphology and mill type on milling induced crystal disorder. Eur. J. Pharm. Sci. 27, 19–26.
Chongprasert, S., Griesser, U.J., Bottorff, A.T., Williams, N.A., Byrn, S.R., Nail, S.L., 1998. Effects of freeze–dry processing conditions on the crystallization of pentamidine isethionate. J. Pharm. Sci. 87, 1155–1160.
Clydesdale, G., Roberts, K.J., Telfer, G.B., Grant, D.J.W., 1997. Modeling the crystal morphology of α-lactose monohydrate. J. Pharm. Sci. 86, 135–141.
Crowley, P., Martini, L., 2001. Drug-excipient interactions. Pharm. Tech. Eur., March 2001, 26–34.
Darcy, P., Buckton, G., 1997. The influence of heating/drying on the crystallisation of amorphous lactose after structural collapse. Int. J. Pharm. 158, 157–164.
Di Martino, P., Martelli, S., Guyot-Hermann, A.-M., Guyot, J.-C., Drache, M., Conflant, P., 1993. The batch-to-batch non reproducibility of the compression ability of lactose. Reasons and detection. S.T.P. Pharma Sci. 3, 436–441.
Dilworth, S.E., Buckton, G., Gaisford, S., Ramos, R., 2004. Approaches to determine the enthalpy of crystallisation, and amorphous content, of lactose from isothermal calorimetric data. Int. J. Pharm. 284, 83–94.
Dincer, T.D., Parkinson, G.M., Rohl, A.L., Ogden, M.I., 1999. Crystallisation of α-lactose monohydrate from dimethyl sulfoxide (DMSO) solutions: influence of β-lactose. J. Cryst. Growth 205, 368–374.
Figura, L.O., Epple, M., 1995. Anhydrous α-lactose. A study with DSC and TXRD. J. Thermal Anal. 44, 45–53.
Fix, I., Steffens, K.-J., 2004. Quantifying low amorphous or crystalline amounts of alpha-lactose monohydrate using X-ray powder diffraction, near-infrared spectroscopy, and differential scanning calorimetry. Drug Dev. Ind. Pharm. 30, 513–523.
Fries, D.C., Rao, S.T., Sundaralingam, M., 1971. Structural chemistry of carbohydrates. III. Crystal and molecular structure of 4-*O*-β-D-galactopyranosyl-α-D-glucopyranose monohydrate (α-lactose monohydrate). Acta Crystallogr. B27, 994–1005.
Fukuoka, E., Makita, M., Yamamura, S., 1993. Preferred orientation of crystallites in tablets. III. Variations of crystallinity and crystallite size of pharmaceuticals with compression. Chem. Pharm. Bull. 41, 595–598.
Fukuoka, E., Terada, K., Makita, M., Yamamura, S., 1995. Paracrystalline lattice distortion in crystalline pharmaceuticals. Determination of paracrystalline lattice distortion by powder X-ray diffraction. Chem. Pharm. Bull. 43, 671–676.
Galwey, A.K., 2000. Structure and order in thermal dehydrations of crystalline solids. Thermochim. Acta 355, 181–238.
Garnier, S., Petit, S., Coquerel, G., 2002a. Influence of supersaturation and structurally related additives on the crystal growth of α-lactose monohydrate. J. Cryst. Growth 234, 207–219.

Garnier, S., Petit, S., Coquerel, G., 2002b. Dehydration mechanism and crystallisation behaviour of lactose. J. Therm. Anal. Cal. 68, 489–502.
Giron, D., 1995. Thermal analysis and calorimetric methods in the characterisation of polymorphs and solvates. Thermochim. Acta 248, 1–59.
Goodhart, F.W., 1994. Lactose. In: Wade, A., Weller, P.J. (Eds.), Handbook of Pharmaceutical Excipients, 2nd ed. The Pharmaceutical Press, London, pp. 252–261.
Görbitz, C.H., Hersleth, H.P., 2000. On the inclusion of solvent molecules in the crystal structures of organic compounds. Acta Crystallogr. B 56, 526–534.
Halttunen, H., Nurmi, J., Perkkalainen, P., Pitkänen, I., Räisänen, S., 1997. Influence of drying to the structure of lactitol monohydrate. J. Thermal Anal. 49, 809–816.
Haque, M.K., Roos, Y.H., 2005. Crystallization and X-ray diffraction of spray–dried and freeze–dried amorphous lactose. Carbohydr. Res. 340, 293–301.
Hüttenrauch, R., 1983. Modification of starting materials to improve tabletting properties. Pharm. Ind. 45, 435–440.
Hüttenrauch, R., Keiner, I., 1979. Produce lattice defects by drying process. Int. J. Pharm. 2, 59–60.
Hüttenrauch, R., Fricke, S., Zielke, P., 1985. Mechanical activation of pharmaceutical systems. Pharm. Res., 302–306.
Irwin, W.J., Iqbal, M., 1991. Solid-state stability: the effect of grinding solvated excipients. Int. J. Pharm. 75, 211–218.
Itoh, T., Satoh, M., Adachi, S., 1977. Differential thermal analysis of α-lactose hydrate. J. Dairy Sci. 60, 1230–1235.
Khankari, R.K., Grant, D.J.W., 1995. Pharmaceutical hydrates. Thermochim. Acta 248, 61–79.
Kirk, J.H., Dann, S.E., Blatchford, C.G., 2007. Lactose: a definitive guide to polymorph determination. Int. J. Pharm. 334, 103–114.
Kumon, M., Suzuki, M., Kusai, A., Yonemochi, E., Terada, K., 2006. Novel approach to DPI carrier lactose with mechanofusion process with additives and evaluation by IGC. Chem. Pharm. Bull. 54, 1508–1514.
Le Bail, A., Duroy, H., Fourquet, J.L., 1988. The *ab-initio* structure determination of lithium antimony tungstate ($LiSbWO_6$) by X-ray powder diffraction. Mater. Res. Bull 23, 447–452.
Lefebvre, J., Willart, J.-F., Caron, V., Lefort, R., Affouard, F., Danede, F., 2005. Structure determination of the 1:1α/β mixed lactose by X-ray powder diffraction. Acta Crystallogr. B61, 455–463.
Lefort, R., Caron, V., Willart, J.-F., Descamps, M., 2006. Mutarotational kinetics and glass transition of lactose. Solid State Commun. 140, 329–334.
Lerk, C.F., Andreae, A.C., de Boer, A.H., de Hoog, P., Kussendrager, K., van Leverink, J., 1984. Alterations of α-lactose during differential scanning calorimetry. J. Pharm. Sci. 73, 856–859.
Lim, S.G., Nickerson, T.A., 1973. Effect of methanol on the various forms of lactose. J. Dairy Sci. 56, 843–848.
Longuemard, P., Jbilou, M., Guyot-Hermann, A.-M., Guyot, J.-C., 1998. Ground and native crystals: comparison of compression capacity and dissolution rate. Int. J. Pharm. 170, 51–61.
Mnyukh, Y.V., 1979. Molecular mechanism of polymorphic transitions. Mol. Cryst. Liq. Cryst. 52, 163–200.
Morita, M., Nakai, Y., Fukuoka, E., Nakajima, S.-I., 1984. Physicochemical properties of crystalline lactose. II. Effect of crystallinity on mechanical and structural properties. Chem. Pharm. Bull. 32, 4076–4083.
Morris, K.R., 1999. Structural aspects of hydrates and solvates. In: Brittain, H.G. (Ed.), Polymorphism in Pharmaceutical Solids, 95. Marcel Dekker, New York, pp. 125–181.
Morris, K.R., Nail, S.L., Peck, G.E., Byrn, S.R., Griesser, U.J., Stowell, J.G., Hwang, S.-J., Park, K., 1998. Advances in pharmaceutical materials and processing. Pharm. Sci. Technol. Tod. 1, 235–245.
Morris, K.R., Griesser, U.J., Eckhardt, C.J., Stowell, J.G., 2001. Theoretical approaches to physical transformations of active pharmaceutical ingredients during manufacturing processes. Adv. Drug Deliv. Rev. 48, 91–114.
Niemelä, P., Päällysaho, M., Harjunen, P., Koivisto, M., Lehto, V.-P., Suhonen, J., Järvinen, K., 2005. Quantitative analysis of amorphous content of lactose using CCD-Raman spectroscopy. J. Pharm. Biomed. Anal. 37, 907–911.
Noordik, J.H., Beurskens, P.T., Bennema, P., Visser, R.A., Gould, R.O., 1984. Crystal structure, polarity and morphology of 4-*O*-β-D-galactopyranosyl-α-D-glucopyranose monohydrate (α-lactose monohydrate): a redetermination. Z. Kristallogr. 168, 59–65.
Otsuka, M., Ohtani, H., Kaneniwa, N., Higuchi, S., 1991. Isomerization of lactose in solid-state by mechanical stress during grinding. J. Pharm. Pharmacol. 43, 148–153.
Petit, S., Coquerel, G., 1996. Mechanism of several solid–solid transformations between dihydrated and anhydrous copper(II) 8-hydroxyquinolinates. Proposition for a unified model for the dehydration of molecular crystals. Chem. Mater. 8, 2247–2258.
Platteau, C., Lefebvre, J., Affouard, F., Derollez, P., 2004. *Ab initio* structure determination of the hygroscopic anhydrous form of α-lactose by powder X-ray diffraction. Acta Crystallogr. B60, 453–460.
Platteau, C., Lefebvre, J., Affouard, F., Willart, J.-F., Derollez, P., Mallet, F., 2005. Structure determination of the stable anhydrous phase of α-lactose from X-ray powder diffraction. Acta Crystallogr. B61, 185–191.
Price, R., Young, P.M., 2004. Visualization of the crystallization of lactose from the amorphous state. J. Pharm. Sci. 93, 155–164.
Raghavan, S.L., Ristic, R.I., Sheen, D.B., Sherwood, J.N., Trowbridge, L., York, P., 2000. Morphology of crystals of α-lactose hydrate grown from aqueous solution. J. Phys. Chem. B 104, 12256–12262.
Raghavan, S.L., Ristic, R.I., Sheen, D.B., Sherwood, J.N., 2001. The bulk crystallization of α-lactose monohydrate from aqueous solution. J. Pharm. Sci. 90, 823–832.
Rodriguez-Carvajal, J., 2001. FULLPROF, version March, 2003, LLB, CEA/Saclay, France.
Roisnel, T., Rodriguez-Carvajal, J., 2001. WinPLOTR: a Windows tool for powder diffraction pattern analysis. Mater. Sci. Forum 378–381, 118–123.
Roos, Y., Karel, M., 1992. Crystallization of amorphous lactose. J. Food Sci. 57, 775–777.
Sebhatu, T., Angberg, M., Ahlneck, C., 1994. Assessment of the degree of disorder in crystalline solids by isothermal microcalorimetry. Int. J. Pharm. 104, 135–144.
Shakhtshneider, T.P., Boldyrev, V.V., 1999. Mechanochemical synthesis and mechanical activation of drugs. In: Boldyreva, E., Boldyrev, V. (Eds.), Reactivity of Molecular Solids. Wiley & Sons, New York, pp. 271–311.
Stephens, P.W., 1999. Phenomenological model of anisotropic peak broadening in powder diffraction. J. Appl. Cryst. 32, 281–289.
Stephenson, G.A., Diseroad, B.A., 2000. Structural relationship and desolvation behavior of cromolyn, cefazolin and fenoprofen sodium hydrates. Int. J. Pharm. 198, 167–177.
Stephenson, G.A., Groleau, E.G., Kleemann, R.L., Xu, W., Rigsbee, D.R., 1998. Formation of isomorphic desolvates: creating a molecular vacuum. J. Pharm. Sci. 87, 536–542.
Thompson, P., Cox, D.E., Hastings, J.B., 1987. Rietveld refinement of Debye–Scherrer synchrotron X-ray data from alumina. J. Appl. Cryst. 20, 79–83.
Van der Sluis, P., Kroon, J., 1989. Solvents and X-ray crystallography. J. Cryst. Growth 97, 645–656.
Van Kreveld, A., 1969. Growth rates of lactose crystals in solutions of stable anhydrous α-lactose. Neth. Milk Dairy J. 23, 258–275.
Vippagunta, S.R., Brittain, H.G., Grant, D.J.W., 2001. Crystalline solids. Adv. Drug Deliv. Rev. 48, 3–26.
Vromans, H., De Boer, A.H., Bolhuis, G.K., Lerk, C.F., Kussendrager, K.D., 1985. Studies on tabletting properties of lactose. Part I. The effect of initial particle size on binding properties and dehydration characteristics of lactose. Acta Pharm. Suec. 22, 163–172.
Walstra, P., Jenness, R., 1984. Carbohydrates. In: Dairy Chemistry and Physics. Wiley and Sons, pp. 27–41.
Willart, J.-F., De Gusseme, A., Hemon, S., Descamps, M., Leveiller, F., Rameau, A., 2002. Vitrification and polymorphism of trehalose induced by dehydration of trehalose dihydrate. J. Phys. Chem. B 106, 3365–3370.
Willart, J.-F., Caron, V., Lefort, R., Danède, F., Prévost, D., Descamps, M., 2004. Athermal character of the solid state amorphization of lactose induced by ball milling. Solid State Commun. 132, 693–696.
Wong, D.Y.T., Waring, M.J., Wright, P., Aulton, M.E., 1991. Elucidation of the compressive deformation behaviour of α-lactose monohydrate and anhydrous α-lactose single crystals by mechanical strength and acoustic emission analyses. Int. J. Pharm. 72, 233–241.
Yajima, K., Okahira, A., Hoshino, M., 1997. Transformation of lactitol crystals and dehydration with grinding. Chem. Pharm. Bull. 45, 1677–1682.